Towards Energetically Autonomous Foraging Soft Robots.

Hemma Philamore[1,3], Ioannis Ieropoulos[2,3], Andrew Stinchcombe[2,3] and Jonathan Rossiter[1,3]

August 10, 2016

Abstract

A significant goal of robotics is to develop autonomous machines, capable of independent and collective operation free from human assistance. To operate with complete autonomy robots must be capable of independent movement and total energy self-sufficiency. We present the design of a soft robotic mouth and artificial stomach for aquatic robots that will allow them to feed on biomatter in their surrounding environment. The robot is powered by electrical energy generated through bacterial respiration within a microbial fuel cell (MFC) stomach, and harvested using state-of-the-art voltage step-up electronics. Through innovative exploitation of compliant, biomimetic actuation, the soft robotic feeding mechanism enables the connection of multiple MFC stomachs in series configuration in an aquatic environment, previously a significant challenge. We investigate how a similar soft robotic feeding mechanism could be driven by electroactive polymer artificial muscles from the same bioenergy supply. This work demonstrates the potential for energetically autonomous soft robotic artificial organisms and sets the stage for radically different future robots.

1 Introduction

There has long been a drive within robotics research to emulate the sophistication and efficiency of biological organisms. This approach has led to the emergence of biomimetic, soft robotic actuators that demonstrate superior performance when compared to their rigid counterparts. Properties of these actuators typically include mechanical redundancy, impact toughness, and multi-degree of freedom actuation, thereby allowing the robot to adapt to its surroundings ([1], [2]). Concurrently, the development of robots that operate with complete autonomy, including energy sustenance [3] has been a major goal in robotics research. Truly autonomous robots have the potential to operate in inhospitable, polluted or hard to reach environments. The energy autonomy capabilities of current robots are far inferior to those of even the most basic biological organisms.
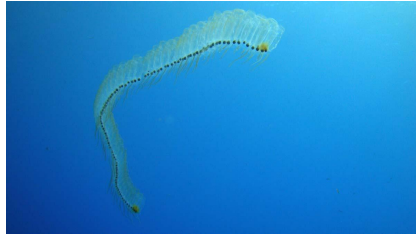
(a) A chain of connected salps. Large chains, exceeding 500mm in length can comprise around 200 individuals [4]. 'Salpenkette auf Gozo bei Malta', Hartmut Olstowski, 2010 , Licensed under CC BY-SA 3.0 via Wikimedia Commons.
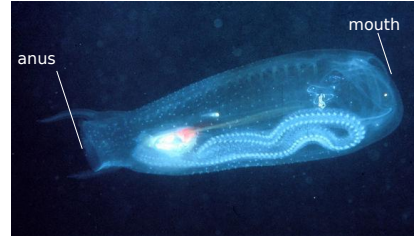
(b) A solitary salp, typical body length >10mm, <100mm ([5]).'Thetys vagina Salp, Solitary Phase', Lovell and Libby Langstroth, 2005, Licensed under CC BY-NO-SA 3.0 via California Academy of Sciences. Original image edited by addition of annotations.

Figure 1: Photographs of salps in their two life phases.

Most robots depend on well established sources of power that limit the range of operation of the robot either by tethered operation, for example pneumatic or hydraulic actuation driven by pumps too large to carry on-board [6], or the requirement to return intermittently to a base-station in the case of robots with re-chargeable batteries [7]. Recent soft robotics research has shown actuation mechanisms driven by environmental stimuli, for example chemical gradients [8] or phototaxis [9]. However, these robots do not store energy for use in lean times, nor do they optimise the way in which this energy is used. The foraging behaviour of natural organisms presents a more promising solution for powering energy autonomous robots. Robots that emulate this behaviour to provide long term energy autonomy in remote environments using scavenged environmental energy include those which use photovoltaic cells ([10],[11]), kinetic energy from the wind or tide ([12],[13]), underwater thermal gradients [14] and fermentation [15] and combustion [16] of biomatter.
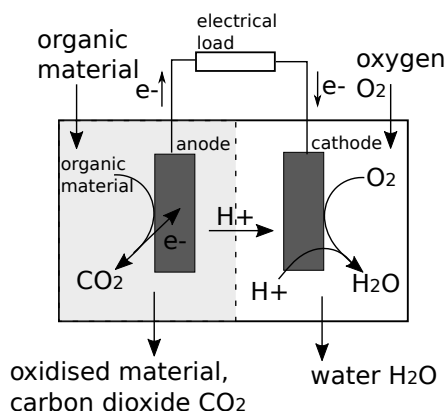
Figure 2: Diagram showing principle of operation of an MFC. Organic matter is oxidised at the anode electrode. Standard reduction and oxidation (redox) potentials generated by oxidation of organic carbohydrates at the anode and reduction of cations at the cathode result in a potential difference across the MFC and the flow of current when the electrodes are connected by a resistive load.

Microbial fuel cells (MFCs), which are used to power robots such as Gastrobot [17] and the EcoBot robot series [18] exploit the metabolism of microbes to break down organic biomass and convert it into electricity. The configuration of an MFC comprises two electrodes which are separated electrically, but allow the intermediate transport of ions (Figure 2). Previous work has demonstrated the use of naturally occurring substrates such as seawater [19], marine and freshwater sediment [20] and waste water [21] as an energy source for MFCs, showing their suitability for powering robots in many different aquatic environments.

Until now the operation of these robots has been limited to within a controlled environment by the use of wheeled locomotion and complex mechanisms to feed from specifically designed dispensers [18]. Additionally, the conductivity of the fluid substrates fed to MFCs can result in the unwanted connection of electrodes in contact with the fluid, limiting their use to power aquatic robots. In contrast to the rigid mechanisms previously used, we demonstrate that by using a soft structure, a simple, low cost mechanism is achieved that allows the connections of multiple MFCs in series in fluid environments.

The objective of this study is therefore to design and test a robot that exploits the energy autonomy that can be afforded to soft robots by use of a bio-inspired MFC energy source and, simultaneously, investigates whether the use of compliant, bio-inspired actuation in place of conventional rigid actuators can be used to improve the suitability of MFC-powered robots for harvesting energy from real-world environments. Previous work has shown the benefits of soft robotics to feeding MFCs in the design of components for fluid transport in an artificial digestive systems [22][30]. Expanding on this, we now consider the design of a bio-inspired mouth for MFC-powered robots, inspired by the salp (Figure 1) and produced from a soft flexible polymer membrane. This novel design is expected to inform future work incorporating an MFC stomach into a completely soft, energy autonomous robot. Past work has considered the use of a sub-mL MFC to drive soft robotic actuation of an ionic polymer metal composite (IPMC) ar-

3

tificial muscle actuator in the design of a soft robotic tadpole [23]. Artificial muscles such as IPMC and shape memory alloy (SMA) are a complementary technology for use with an MFC power source due to low drive voltages (1-3V) and high biocompatibility [24]. IPMCs create a bending actuation due to the migration of mobile cations and water molecules. Shape memory alloys (SMA) exhibit thermal transition from the austenitic phase, where the material has a highly elastic structure and assumes its permanent shape, to the martensitic phase where it can be deformed into a temporary shape by application of external stress [25]. As preliminary study we evaluate the mechanical output of these soft thermally and ionically active actuators, driven from the energy harvested from the MFC artificial stomach. This research contrasts with previous work on MFC-powered robots by showing the potential for total energy autonomy using a single MFC.

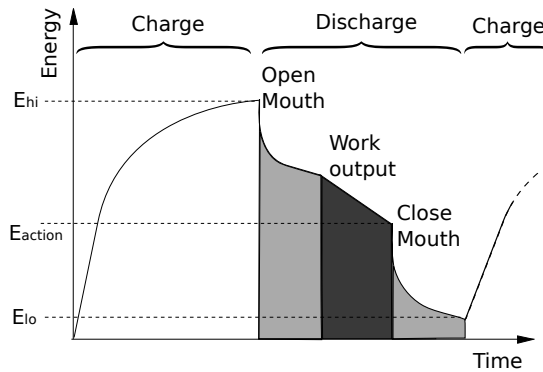## 1.1 Energy Cycle of the Foraging Behaviour

Figure 3: Graph showing the two-phase (charge and discharge) anticipated behavioural cycle of a foraging robot. The robot charges (charge phase is shown in white) until the energy reaches threshold E_{hi}. Then it discharges (the discharge phase is shown in grey, with light grey representing the critical operations for energy sustenance and dark grey representing use of the net energy of the system for useful work). When its energy level falls to a low state, E_{lo}, all energy discharge is halted, allowing charge accumulation to begin again as the organic material is digested. Any surplus energy can be used for goal-directed operations such as sensing and communication, controlled by intermediate thresholds, for example E_{action}.

The simple behaviour cycle for a soft foraging robot with an MFC stomach is shown in Figure 3. The anticipated operation of the robot during the discharge is to open its mouth, move, and then close its mouth, having ingested a fresh batch of feedstock from which it harvests energy during the charge cycle.

We firstly describe the design of the device used in the study (Section 2). Three areas are evaluated; the power production of the MFC, the energy harvested from the MFC and the use of this energy to drive conventional motors and electroactive soft actuators. The experimental method for these investigations is set out in Section 3, followed by a discussion of the results in Section 4. Finally we present the conclusions of the study (Section 5).
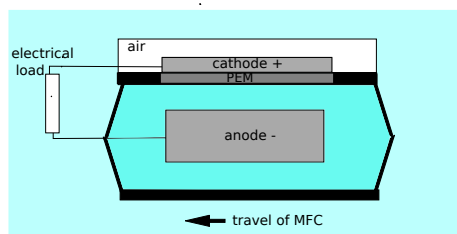
4

2 Foraging Robot Design
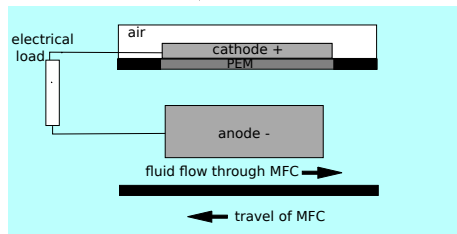
(a) MFC with the cathode electrically isolated from the fluid surrounding the MFC by an air chamber. The anode is electrically connected to the surrounding fluid.
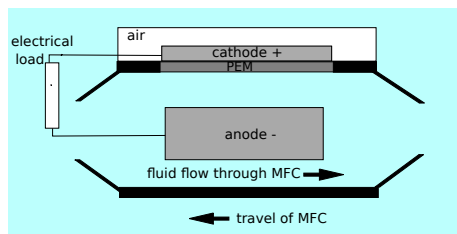
(b) MFC with a mouth mechanism at each end of the anode chamber and with the cathode electrically isolated from the fluid surrounding the MFC by an air chamber. When the mouth is open, as shown, the anode is electrically connected to the fluid surrounding the MFC.


(c) MFC with a mouth mechanism at each end of the anode chamber and with the cathode electrically isolated from the fluid surrounding the MFC by an air chamber. When the mouth is closed, as shown, the anode is electrically isolated from the fluid surrounding the MFC.

Figure 4: Schematic showing 2D cross-section of an MFC in which anolyte is replenished by inflow and outflow of fluid through orifices at each of the anode chamber. The surrounding fluid in which the MFC is submerged is shown as a shaded area around the MFC. The figure is not to scale.

The proposed foraging robot is inspired by the salp which exist either in solitude or as a connected chain of many organisms (Figure 1). A simple replication of this organism would be an MFC at the surface of the water, with the anode submerged and the cath-

ode exposed to the overlying air (Figure 4(a)). However, this prevents the connection of multiple MFCs electronically in series, a widely used strategy for voltage multiplication, due to the unwanted electrical connection by the surrounding fluid. By implementing a mouth-like open-and-close mechanism (Figure 4(b)) the individual MFC anodes are isolated when the opening is closed (Figure 4(c)), allowing operation of the MFC-powered robots either as individual units or in series electrical configuration.

2.1 Design of the Mouth
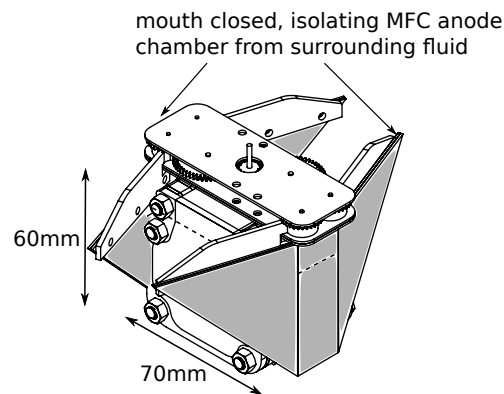
(a) Robot with mouth closed, isolating the anode from the surrounding fluid.
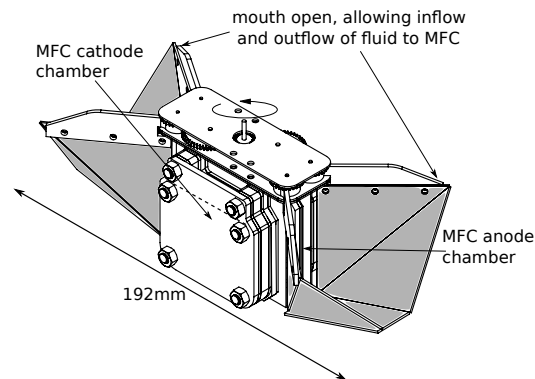
(b) Robot with mouth open, allowing fluid inflow and outflow to the anode chamber.

Figure 5: CAD drawing showing key components of the design for a robot with MFC stomach fed by a soft, bio-inspired mouth mechanism, which is shaded in grey. The approximate water level is indicted by the dotted lines in each figure. The cathode chamber isolates the cathode electrode from the surrounding fluid and exposes it to the overlying air.

6

The robotic MFC floated at the water surface. The mouth mechanism was inspired by the suction feeding of vertebrate fish, which involves expansion of the intra-oral cavity in order to transport food-rich fluid into their mouths [26]. Origami folding of a single soft acetate membrane (thickness = 240 μm approx.) (Figure 5) was used to open the mouth, drawing in the surrounding fluid with suspended particulate matter (Figure 5(b)), and close the mouth, raising the lips of the mouth above the water level (Figure 5(a)). Using this low cost (<£0.5), simple, lightweight, mechanism, the MFC can be fed directly from its fluid surroundings. In contrast to the use of rigid components, use of a soft membrane allowed electrical isolation of the anode chamber from the surrounding fluid when the mouth is closed, without the need for joints or seals. This isolation permits voltage multiplication by series connection of individuals in a configuration, resembling a chain of connected salps.

For repeatability in testing the novel mechanism, the corner folds of the soft membrane were gear coupled to a single central motor drive using rigid plastic components. The MFC cathode chambers were produced from acrylic to replicate the design of an analytical style MFC, enabling direct comparison of the performance of the novel feeding mechanism with this well-established design. For example, recent work has shown 5J per batch of food administered can be generated using this type of analytical-style MFC [27].
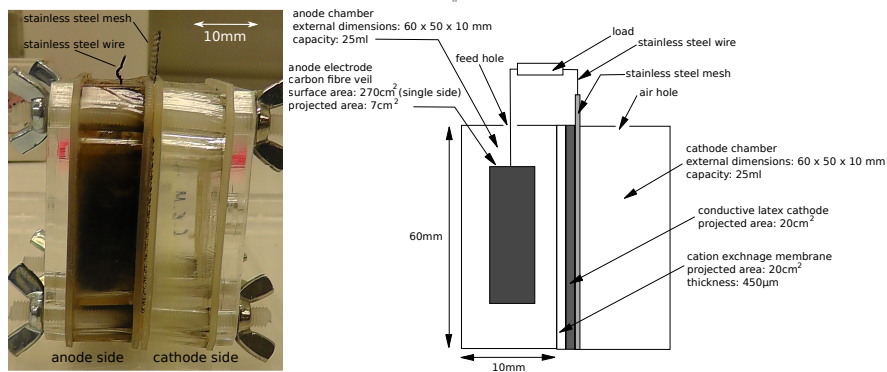
(a) Photograph of MFC in open circuit mode, meaning there is no electrical connection between anode and cathode electrodes.

(b) Schematic detailing the components of the MFCs used in this study. A conductive latex cathode was used to maintain a continuous redox reaction without the need to hydrate the cathode electrode. A polyurethane-based rubber coating (Plasti-Dip, Petersfield UK) was mixed with white spirit and micronised graphite powder in the mass ratio 2:3:1, using a method derived from [28] and painted onto the air side of the membrane. The MFC is configured with an electrical load connecting the anode and cathode electrodes.

Figure 6: An analytical style MFC used as the control experiment in this study and, therefore, on which the design of the MFC with mouth was based.

2.2 The Energy Balance

To achieve the energy autonomy, it was critical that the feeding mechanism could be actuated without energy consumption in excess the energy budget defined by the MFC stomach stomach used to power it.

$$E_{mfc} \geqslant W_{body} \tag{1}$$

where E_{mfc} is the energy generated by the MFC and W_{body} is the mechanical work done by the body, including supply of energy to the MFC. Additionally, the electrical energy harvested, $E_{harvested}$, and the electrical energy consumed, E_{body}, depend on the efficiency of the energy harvesting hardware and motors, respectively. Therefore we can re-define Equation (1) as

$$E_{harvested} \geqslant E_{body} \qquad (2)$$

The work, W_{body} (Table 1), to drive the mouth mechanism, was evaluated experimentally by using a DC motor (AMAX12, Maxon) to drive the central input gear. The work done was found by integrating the power P_{mech} over the opening and closing strokes respectively using the product of the motor torque τ and motor angular velocity ω.

$$W_{body} = \int_{t_i}^{t_f} P_{mech} dt = \overline{\omega} \int_{t_i}^{t_f} \tau dt \qquad (3)$$

A potentiostat (Hokuto Denko) was used to set a voltage and measure the current drawn by the motor at that voltage. The torque was derived from the current drawn by the motor.

Based on previous work using analytical style MFCs (Figure 6), E_{mfc} can be estimated as 5J [27]. W_{body} can be estimated as $W_{open} + W_{close}$ (Table 1). This suggests that Equation (1) may be satisfied, showing the potential of the robot for energy autonomous operation. However, the energy consumed in actuating the motors, E_{body}, due to the efficiency the DC motor used, means that Equation (2) cannot be satisfied. Therefore, the next stage is to firstly, evaluate the energy output by an MFC with the novel design for a soft bio-inspired mouth, in comparison to a conventional analytical style MFC.

Henceforth, we term the MFC with the mouth the 'artificial stomach' to distinguish it from the conventional analytical style MFC, termed the 'control MFC'. Based on this performance verification, suitable actuators and energy harvesting hardware must be sourced to produce a design for an energy autonomous robot, powered by the MFC stomach, by satisfying Equation (2).

Table 1: The electrical energy consumed, $E_{body} = E_{open} + E_{close}$, to supply the mechanical work $W_{body} = W_{open} + W_{close}$, to actuate the mouth, and the resulting first law thermodynamic efficiency η.

	W_{body} (J)	E_{body}, (J)	η (%)
Open	0.04	1.4	2.86
Close	0.16	4.19	3.82

3 Experimental Method

3.1 Power Production From MFCs

Two identical analytical style MFCs were set up (Table 2). One was converted to the artificial stomach with the soft mouth and the other was used as the control. A servo motor (Carson) was initially used to drive the feeding actuation. An Uno microcontroller board (Arduino) was used to control actuations of the robotic MFC, using

manual input switches. The energy required by this system to actuate the mouth and transport the robot was 345.37J.
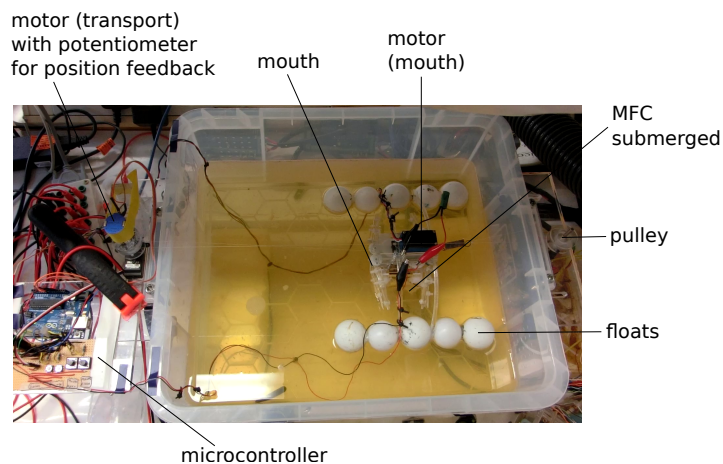

Figure 7: Photograph of the artificial organism in a container of fluid

The foraging robot which was partially submerged in a container of 10L of fluid (Figure 7) of the same composition as the anolyte (Table 2).

The composition of the fluid was chosen to replicate that used in previous work [27] demonstrating power production from MFCs of this type.

The MFCs were batch fed, which involved intermittently replenishing the anode chamber contents using the mouth in the case of the artificial stomach and a syringe for the control. The trigger for administration of a new batch feed was a decrease in MFC power output to $<1~\mu$W. The operations used to feed the artificial stomach over 25 batches of feeding (days 45-401) are shown in Figure 8.

Table 2: Experimental method using two identical analytical style MFCs. A single batch feed involved removing 25ml anolyte using a syringe and replacing it with 25ml of 5mM acetate solution, mixed with 0.2% tryptone, 0.1% yeast extract.
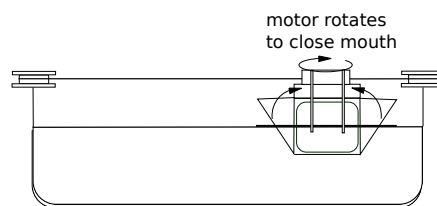
Day	Operation
0	Two analytical style MFCs inoculated: sewage sludge (Wessex Water, Saltford UK) mixed with 2.5% nutrient broth. 10kΩ load. Data logger: LXI data acquisition/switch unit (Agilent Technologies).
0 - 12	Every 2nd day: 5ml anolyte removed, replaced with 5ml stock solution (25mM acetate solution, mixed with 1% tryptone, 0.5% yeast extract).
12	Batch 1, 10kΩ load applied
20	Batch 2, 1kΩ load applied (optimum load for MFCs of this type, [27] to imitate fixed load of EH4295 Micropower Step Up Low Voltage Booster)
33	Batch 3, 1kΩ load applied
45	One of the two analytical style MFCs dismantled. Anode, cathode and cation exchange membrane converted to MFC with mouth.
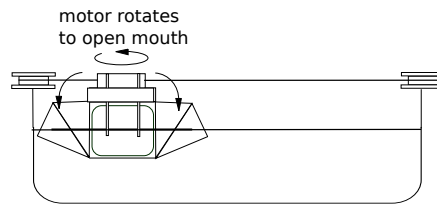
(a) Mouth opens (17s) then remains open for further 3 minutes.
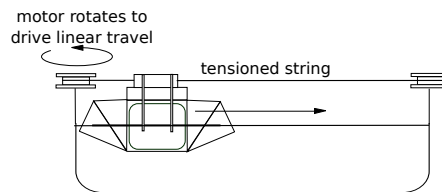
(b) Artificial stomach with mouth transported 20cm linearly at a velocity of $2.5ms^{-1}$ across container of fluid, with mouth open, by rotation of second servo motor fixed to periphery of container. Rotary potentiometer coupled to second servo motor for position feedback to microcontroller. The mouth then remains open for a further 1 minute. Direction of travel alternated with each feed.

(c) Mouth closes (17s)

10

Figure 8: Operations used to feed the artificial stomach. The surrounding fluid in the container was replenished prior to each feed.

The artificial stomach was also fed without transporting it across the container using the rotation of a motor as shown in Figure 8(b) over 2 batches (19 and 20) to evaluate the necessity to travel across the container as a feeding operation.

3.2 Harvesting Energy from MFCs

Energy harvesting circuitry was sourced to store the low output voltage of the MFC-stomach at a boosted voltage for use in feeding an energy autonomous, soft robot. DC motors were sourced to drive the actuation of the soft robot with sufficient efficiency that $E_{body} < E_{harvested}$, satisfying Equation (2) and showing the potential of the robot for energetic autonomy.

While a number of examples of energy harvesting from MFCs using ultra-low voltage input circuits are demonstrated in the literature ([29], [30], [31]), the range of energy harvesting hardware available to MFC technology remains severely limited [32]. As it stands, the current state of the art in commercially available low power voltage step-up technology is represented by the EH4295 inductor-based voltage booster (Advanced Linear Devices Inc). The device outputs AC voltage with a gain between 7 and 10 and has a lower input voltage threshold of 60mV. It has a nominal impedance of 950 Ω. This voltage booster was used to increase the low voltage output of the MFC and an energy harvesting board (EH300, Advanced Linear Devices Inc) was used to rectify the AC output of the voltage booster to a DC voltage, enabling the charge of a storage capacitor (Section 3.2).
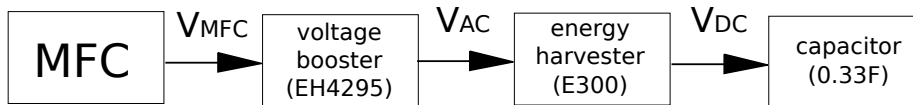
Figure 9: Block diagram of hardware

## 3.3 Powering Actuators Using Harvested Energy

3.3.1 Powering DC motors

To demonstrate the potential of the robot for energy autonomous operation, high efficiency DC motors and gearheads (RE 10 & GP 10 K (Maxon), 16C18, & M915L61(Portescap)) were selected to actuate a replicate of the foraging robot, identical to the design shown in Figure 5, which contained no microbes. The motors were powered by the discharge of 3 x 1F super- capacitors (PowerStor, B series) charged in series to 4.0V (2.64J); the mean recorded energy harvested from the MFC stomach, at this time. Manual switching was used to control the supply of charge to the motors.

3.3.2 Powering IPMC Artificial Muscle

The motors were powered by the discharge of 3 x 1F super- capacitors charged in series to 5.5V (5J), representing the typical energy output of a batch fed, analytical style MFC [27]. The amplification, for example by boost conversion, and associated energy loss due to efficiency, required to achieve this voltage using typical MFC output, was neglected in these experiments. The capacitor was discharged to an IPMC actuator via a MOSFET H bridge circuit (Figure 10) which cycled the charge between opposing

polarities at a frequency of 1Hz. A micro-controller (PIC12LF1822, Microchip) was used to control the switching and was powered in parallel with the IPMC from the discharge of the capacitor. The IPMC strip of length 2.5cm and width 1cm, made from Nafion 117(DuPont), was electroless plated with gold electrodes using the the impregnation reduction fabrication method described in [33]. The Nafion 117 layer had a thickness of 180 microns and the electrode thickness was estimated as 10 microns based on previous work in [34]. The IPMC was fixed with a copper connection at one end. Cantilever actuation of a point at L=1.49cm (Figure 10(a)) from the fixed end was measured using a laser displacement sensor (Keyence LK-G150).
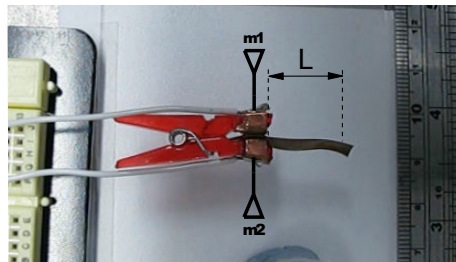
(a) Experimental setup for evaluation of IPMC actuator, viewed from above. L = length of fixed end to point measured by laser displacement sensor. m1 and m2 are connected to the driving electrical circuit shown in Figure 10(b)
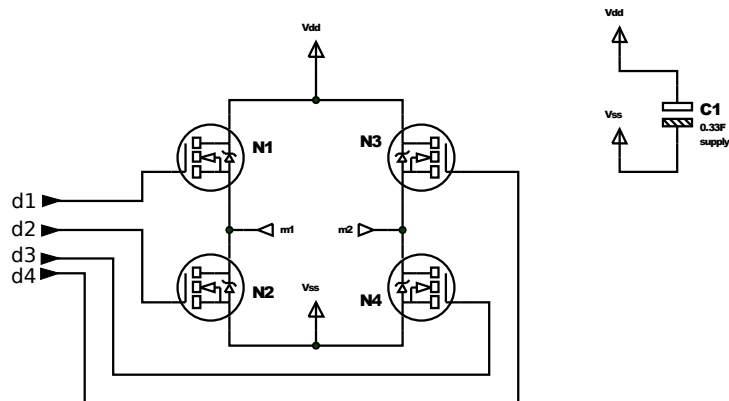
(b) Schematic of electrical circuit driving IPMC actuation. The h-bridge comprised of 4 N-channel, enhancement mode MOSFETs (N1-4), switched by digital output of microcontroller (d1-4)

Figure 10: Experimental set-up for IPMC actuation.

3.3.3 Powering SMA Artificial Muscle

A mass of 3g was suspended vertically by a helical shape memory wire actuator (BioMetal helix, Toki Corp.) of wire diameter (0.15mm) and spring diameter (0.62 mm) and an equilibrium length of 21.6mm. The 3 x 1F super- capacitors charged in series to 5.5V (5J) were discharged directly to the SMA actuator (Figure 16).
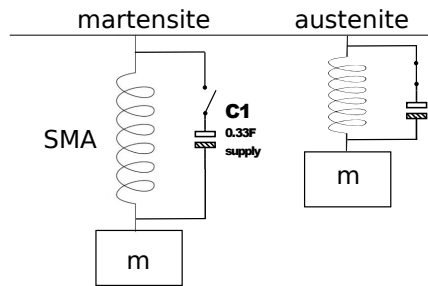
Figure 11: Schematic of SMA actuation driven from direct discharge of supply capacitor C1.

4 Results and Discussion

4.1 Power Production from MFCs

Prior to converting one of the two analytical style MFCs to the artificial stomach design, similar performance (peak power = 18.0μW and 21.45μW respectively, under $1k\Omega$, mean of batches 2-3) was shown by the MFCs.)

Following conversion, continued similarity was shown between the performance of the artificial stomach and the control MFC (10.40 J energy per batch, peak power = 22.86μ W, and 10.57J energy per batch, peak power of 24.50μW, respectively, averaged over 6 batches). This demonstrated that the novel mode of feeding was effective and that MFC performance improved temporally. However, difference between the cycles of the two MFC types can be seen clearly in Figure 12. This may indicate that the difference in feeding mode can impact the peak power output from the MFC.
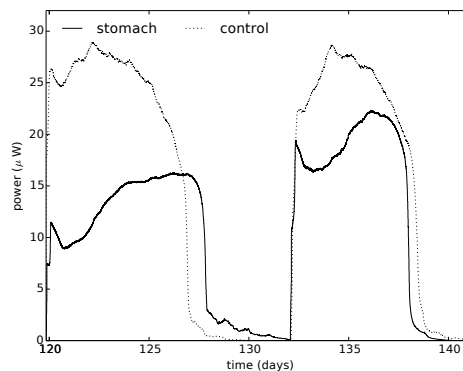

Figure 12: Output from control MFC and foraging robot under 1k Ω load, two batches shown as an example: batches 6 and 7 (begin day 119 and day 132 respectively)
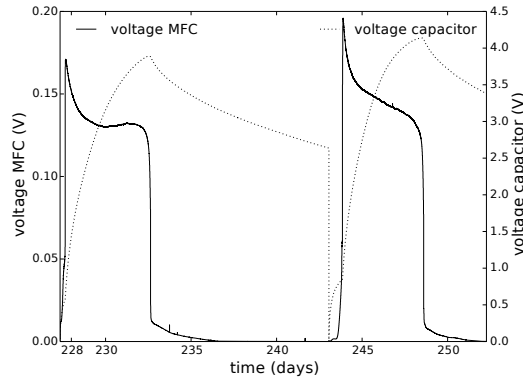
4.2 Harvesting Energy from MFCs

Figure 13: Voltage output from the artificial stomach to the input of the boost converter (load 950 Ω), and the voltage of storage capacitor, charged by the rectified output of the boost converter. Two batches are shown as an example: batches 17 and 18 (beginning day 227 and 243 respectively)

The voltage output of the MFC, when connected to the boost converter and stepped up to the DC-regulated output voltage of the boost converter, charged the 0.33F capacitor connected to the output of the boost converter, as shown in Figure 13. The capacitor was charged to approximately 2.86 J of stored energy per batch (average of three batches) showing an average energy conversion efficiency of 30%. No significant difference in power output was observed when the artificial stomach was not transported across the container of fluid in between opening and closing the mouth (2.87 J of stored energy per batch, average energy conversion efficiency of 29% (average of two batches). This negative result is interesting as it shows that the only actuation required to replenish the contents of the MFC stomach is to open and close the mouth. Therefore, the energy production required of the MFC to achieve energy autonomy is less than initially expected as it does not need to power transport in addition to the mouth.

4.3 Powering Actuators Using Harvested Energy

4.3.1 Powering DC motors

The energy consumed, E_{body}, to actuate the mouth and transport the robot was 1.81J, which satisfied the Equation (2) where the input energy, $E_{harvested}$, was 2.64J.
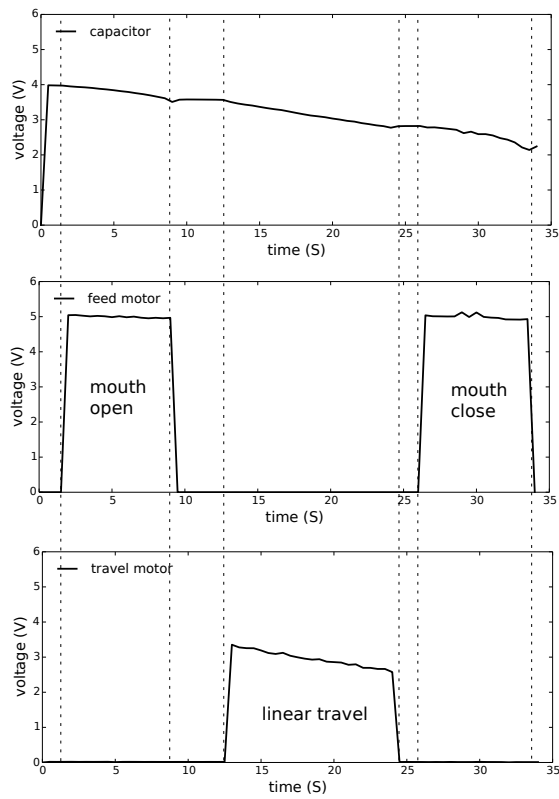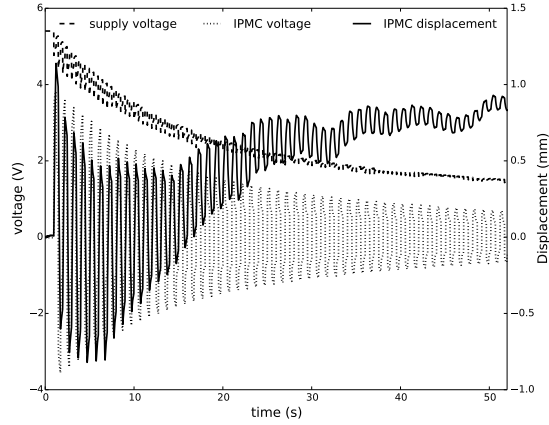
Figure 14: Direct discharge of 0.33 F capacitor charged to 4.0V to two DC motors to drive feeding and travel actuation respectively via an externally powered switching circuit. The voltage of the capacitor (top), and motors that drive the mouth (middle) and the transportation (bottom) are shown.

4.3.2 Powering IPMC Artificial Muscle

The peak to peak amplitude of displacement decreased from 1.74mm to 0.10mm over 104 actuations in 52 seconds (Figure 15(a)), before the capacitor was discharged to below the minimum operating voltage of the micro-controller (1.2V).

(a) Results from start of experiment to time = 52s
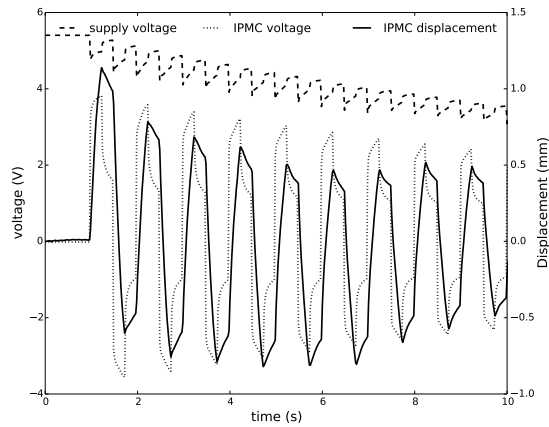
(b) Results from start of experiment to time = 10s

Figure 15: The supply voltage from the capacitor, the voltage across of the IPMC actuator and the cantilever displacement, during discharge of 0.33F capacitor, charged to 5.5V into IPMC artificial muscle, via a simultaneously power switching circuit, with a switching frequency of 1 Hz.

The bending moment, M, generated by the first actuation of the IPMC, was found by $M = \frac{2yIE}{L^2}$ as 701 μNm , where y is the deflection of a point at length, L, from the fixed end of the IPMC and I and E are, respectively, the equivalent moment of inertia and Young's modulus of the IPMC. The energy consumed from the capacitor per stroke, $E_{elec} = \frac{1}{2}CV_{n-1}^2 - \frac{1}{2}CV_n^2$, where V_{n-1} and V_n are the voltage of the capacitor of size C prior to and following actuation, decreased from 182mJ to 2mJ over 104 strokes. This showed that energetic IPMC oscillation can be driven from the typical energy output of an MFC. This may have application in future development of an MFC-powered soft robot.

16

4.3.3 Powering SMA Artificial Muscle

An instantaneous drop in voltage of the supply capacitor (5.5V to 4.0V) indicated the relatively large initial current drawn by the SMA actuator. The SMA contracted to a length of 17.8mm due to the charge from the capacitor Figure 16(a) with a peak force, F = 29mN. The actuator reaches its fully contracted state within 500ms (Figure 16(b)).

(a) Results from start of experiment to time = 52s
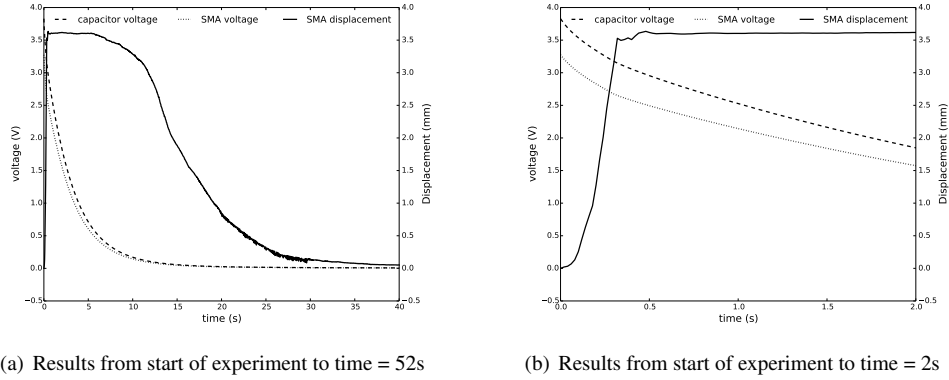

(b) Results from start of experiment to time = 2s

Figure 16: The supply voltage from the capacitor, the voltage across of the SMA actuator and the displacement of the suspended mass during discharge of 0.33F capacitor, charged to 5.5V into SMA artificial muscle.

During the initial contraction, the first law thermodynamic efficiency η was found to be 0.2% by $\eta = \frac{W_{mech}}{E_{elec}} = \frac{\int_0^t F v dt}{\frac{1}{2}CV_{n-1}^2 - \frac{1}{2}CV_n^2}$ where $W_{mech} = \int_0^t F v dt$, F is axial force v is linear velocity, and E_{elec} is the energy consumed from the capacitor. The force and displacement output may be employed in the design of a robot combining the advantageous characteristics of both soft robotics and MFC power, however these benefits may come at the price of reduced thermodynamic efficiency.

5   Conclusion

The development of an MFC artificial stomach, with a soft robotic mouth, has shown great potential to increase the energy autonomy with which aquatic robots can operate. Additionally it may expand the application of MFCs in aquatic environments due to electrical isolation of the anode chamber. This entirely new mechanism for feeding a novel power source will enable increased use of soft robots in real world aquatic environments. In this study, the materials and dimensions of the MFC design were chosen so that the performance of novel design features (the mouth) may be directly evaluated against the results of previous work using the same configuration of MFC [27]. However, future work may include adapting the design of the artificial stomach to include features that related work has shown to improve MFC performance in terms of increased energy output ([35], [36]). Additionally, replacing rapid fabrication with higher precision techniques may be a way to improve the mechanical efficiency of operation, for example through better component alignment and reduced friction. The use of soft robotic actuators, such as the IPMC and SMA artificial muscles presented in this

work, may be instrumental in improving the real world survivability of the design of the robot, by replacing the complex, multicomponent, rigid actuators. However, there is a likely trade-off between mechanical robustness and thermodynamic efficiency, as shown by the lower efficiency operation of the IPMC actuator in this study (0.2% compared to 2.86-3.83% (DC motor)). High efficiency, low power control is a current them of our work towards achieving full energetic autonomy of the foraging soft robot. Additionally, our future work will investigate the use of a soft mouth to feed a totally soft robot. This work makes a significant contribution to soft and MFC-powered robotics, by their combined use in a completely novel aquatic robot.

[1]Dept. of Engineering Mathematics, University of Bristol, Bristol, UK
[2]Bristol BioEnergy Centre, University of the West of England, Bristol, UK
[3]Bristol Robotics Laboratory, Bristol, UK

References

[1] C Laschi, B Mazzolai, V Mattoli, M Cianchetti, and P Dario. Design of a biomimetic robotic octopus arm. *Bioinspiration & biomimetics*, 4(1), 2009.

[2] R F Shepherd, F Ilievski, W Choi, S a. Morin, a. a. Stokes, a. D Mazzeo, X Chen, M Wang, and G M Whitesides. From the Cover: Multigait soft robot. *Proceedings of the National Academy of Sciences*, 108(51):20400–20403, 2011.

[3] David McFarland and Emmet Spier. Basic Cycles, Utility and Optimism in Self-Sufficient Robots. *Robotics and Autonomous Systems*, 20:179–190, 1997.

[4] G R Harbison and R W Gilmer. The feeding rates of the pelagic tunicate, Pegea confoederata and two other salps. *Limnology and Oceanography*, 21:517–528, 1976.

[5] Sunwoo Kim, Jung-Hye Won, and Chang-Bae Kim. Taxonomic Study of Genus Cyclosalpa (Thaliacea: Salpida: Salpidae) from Korea. *Animal Systematics, Evolution and Diversity*, 28(4):261–268, 2012.

[6] Kurt S Aschenbeck, Nicole I Kern, Richard J Bachmann, and Roger D Quinn. Design of a quadruped robot driven by air muscles. *Proceedings of the First IEEE/RAS-EMBS International Conference on Biomedical Robotics and Biomechatronics, 2006, BioRob 2006*, 2006:875–880, 2006.

[7] Von Howard Ebron, Zhiwei Yang, Daniel J Seyer, Mikhail E Kozlov, Jiyoung Oh, Hui Xie, Joselito Razal, Lee J Hall, John P Ferraris, Alan G Macdiarmid, and Ray H Baughman. Fuel-powered artificial muscles. *Science (New York, N.Y.)*, 311(5767):1580–3, 2006.

[8] Martin Hanczyc. Droplets: Unconventional Protocell Model with Life-Like Dynamics and Room to Grow. *Life*, 4(4):1038–1049, 2014.

[9] M P M Dicker, J M Rossiter, I P Bond, and P M Weaver. Biomimetic photo-actuation: sensing, control and actuation in sun-tracking plants. *Bioinspiration & biomimetics*, 9(3):36015, 2014.

[10] L. Ray, A. Price, A. Streeter, D. Denton, and J.H. Lever. The Design of a Mobile Robot for Instrument Network Deployment in Antarctica. *Proceedings of the 2005 IEEE International Conference on Robotics and Automation*, 34(4):2111–2116, 2005.

[11] Mars Exploration Rover Landings Press Kit. Technical Report January, NASA, 2004.

[12] G A Hajos, J A Jones, A Behar, M Dodd, Jack Jones, Aerospace Engineer, Missions Branch, Senior Principal Engineer, Advanced Thermal, Mobility Technologies, Senior Technical Staff, and Robotic Vehicles Group. An Overview of Wind-Driven Rovers for Planetary Exploration. pages 1–13, 1998.

[13] Etienne Gernez, Cesar Minoru Harada, Rik Bootsman, Zenon Chaczko, Gabriella Levine, and Peter Keen. Protei open source sailing drones: A platform for education in ocean exploration and conservation. *2012 International Conference on Information Technology Based Higher Education and Training (ITHET)*, pages 1–7, 2012.

[14] R.E. Davis, C.C. Eriksen, and C.P. Jones. Autonomous buoyancy-driven underwater gliders. In Gwyn Griff, editor, *The Technology and Applications of Autonomous Underwater Vehicles*, pages 37–58. Taylor and Francis, London, 2002.

[15] John Greenman, Owen Holland, Ian Kelly, Kevin Kendall, David McFarland, and Chris Melhuish. Towards robot autonomy in the natural world: a robot in predator's clothing. *Mechatronics*, 13(3):195–228, 2003.

[16] Brief Project Overview Eatr : Energetically Autonomous Tactical Robot. Technical report, DARPA.

[17] Stuart Wilkinson. " Gastrobots "— Benefits and Challenges of Microbial Fuel Cells in Food Powered Robot Applications. *Autonomous Robots*, 9:99–111, 2000.

[18] Ioannis Ieropoulos, John Greenman, Chris Melhuish, and Ian Horsfield. EcoBot-III : a robot with guts. In *Proceedings of the Alife 7 Conference*, pages 733–740, 2010.

[19] Clare E Reimers, Hilmar A Stecher Iii, John C Westall, Yvan Alleau, Kate A Howell, Leslie Soule, Helen K White, and Peter R Girguis. Substrate Degradation Kinetics , Microbial Diversity , and Current Efficiency of Microbial Fuel Cells Supplied with Marine Plankton Substrate Degradation Kinetics , Microbial Diversity , and Current Efficiency of Microbial Fuel Cells Supplied with Marine. *Applied and Environmental Microbiology*, 2007.

[20] Daniel a. Lowy and Leonard M Tender. Harvesting energy from the marine sediment–water interface. *Journal of Power Sources*, 185(1):70–75, oct 2008.

[21] P. Aelterman, K. Rabaey, P. Clauwaert, and W. Verstraete. Microbial fuel cells for wastewater treatment. *Water Science & Technology*, 54(8):9, 2006.

[22] Ioannis Ieropoulos, Iain Anderson, Todd Gisby, Cheng Hung Wang, and Jonathan Rossiter. Microbial-powered artificial muscles for autonomous robots. In *Taros Autonomous Robotic Systems*, number September, pages 209–216, 2008.

[23] Ieropoulos I Philamore H, Rossiter J. An Energetically-Autonomous Robotic Tadpole with Single Membrane Stomach and Tail. In *Proc Biomimetic and Bio-hybrid Systems, 4th international conference, Living Machines, LNAI 9222*, pages 366–378, 2015.

[24] Mohsen Shahinpoor and Kwang J Kim. Ionic polymer–metal composites: IV. Industrial and medical applications. *Smart Materials and Structures*, 14(1):197–214, 2004.

[25] Andreas Lendlein and Steffen Kelch. Shape-Memory Polymers. *Angew. Chem. Int. Ed.*, 41(12):2034–2057, 2002.

[26] Mark W Westneat. Skull biomechanics and suction feeding in fishes. In George V Lauder Robert E. Shadwick, editor, *Fish Physiology: Fish Biomechanics*, pages 29–69. Academic Press, 2006.

[27] Hemma Philamore, Jonathan Rossiter, Peter Walters, Jonathan Winfield, and Ioannis Ieropoulos. Cast and 3D printed ion exchange membranes for monolithic microbial fuel cell fabrication. *Journal of Power Sources*, 289:91–99, 2015.

[28] Jonathan Winfield, Lily D Chambers, Andrew Stinchcombe, and Jonathan Rossiter. The power of glove : Soft microbial fuel cell for low-power electronics. *Journal of Power Sources*, 249:327–332, 2014.

[29] Deukhyoun Heo. Batteryless , Wireless Sensor Powered by a Sediment Microbial Fuel Cell. *Environmental science & technology*, 42(22):8591–8596, 2008.

[30] Daxing Zhang, Fan Yang, Tsutomu Shimotori, Kuang Ching Wang, and Yong Huang. Performance evaluation of power management systems in microbial fuel cell-based energy harvesting applications for driving small electronic devices. *Journal of Power Sources*, 217:65–71, 2012.

[31] Nicolas Degrenne, Bruno Allard, Francois Buret, Florent Morel, Salah-Eddine Adami, and Denis Labrousse. Comparison of 3 self-starting step-up DC:DC converter topologies for harvesting energy from low-voltage and low-power microbial fuel cells. *Proceedings of the 2011 14th European Conference on Power Electronics and Applications*, pages 1–10, 2011.

[32] Andrew Meehan, Hongwei Gao, Senior Member, and Zbigniew Lewandowski. Energy Harvesting With Microbial Fuel Cell and Power Management System. *IEEE Transactions on Power Electronics*, 26(1):176–181, 2011.

[33] Naoko Fujiwara, Kinji Asaka, Yasuo Nishimura, Keisuke Oguro, and Eiichi Torikai. Preparation of gold-solid polymer electrolyte composites as electric stimuli-responsive materials. *Chemistry of Materials*, 12(6):1750–1754, 2000.

[34] Mohsen Shahinpoor and Kwang J Kim. *Ionic polymer – metal composites : I .*, volume 819. 2001.

[35] Peter Aelterman, Korneel Rabaey, Hai The Pham, Nico Boon, and Willy Verstraete. Continuous Electricity Generation at High Voltages and Currents Using Stacked Microbial Fuel Cells. *Environmental Science & Technology*, 40(10):3388–3394, 2006.

[36] Ioannis Ieropoulos, John Greenman, Chris Melhuish, and John Hart. Energy accumulation and improved performance in microbial fuel cells. *Journal of Power Sources*, 145(2):253–256, aug 2005.